Sixth International Symposium on Turbulence and Shear Flow Phenomena
Seoul, Korea, 22-24 June 2009

THE NEAR AND INTERMEDIATE FIELD OF A ROUND FREE JET: THE EFFECT OF REYNOLDS NUMBER AND MIXING TRANSITION

Hachimi Fellouah and Andrew Pollard

Department of Mechanical and Materials Engineering

Queen's University at Kingston

Ontario, K7L 3N6 CANADA

{fellouah, pollard@me.queensu.ca}

ABSTRACT

Flying and stationary hot wire measurements were made to investigate the effect of the Reynolds number on the near and intermediate fields, ($0 \leq x/D \leq 25$), of a round free jet. Measurements were carried out over a range of Reynolds numbers, based on the jet exit mean velocity and the nozzle diameter, that span the mixing transition. The specific Reynolds numbers tested were 6,000, 10,000, 30,000, 50,000 and 100,000. The objective of this study was to outline the variation of the different micoscales in the near and intermediate-fields.

Results showed that the length of the potential core region decreases with increasing the Reynolds number. The axial mean velocity reaches the self-similar state faster than the turbulence intensities. The range of frequencies that comprise the inertial sub-range increases with distance downstream from the jet inlet. The Reynolds number range considered clearly pointed to a mixing transition at Reynolds numbers above *~20,000*. This was accompanied by the appearance of the inertial subrange. At Reynolds numbers below the mixing transition, the energy of the large scale turbulence proceeds directly to the dissipation range. Considering the energy spectra distribution and the development of the different length scales, the mixing transition was found to be a local phenomenon.

INTRODUCTION

This paper owes its origins to the seminal paper by Ricou and Spalding (1961), which identified that entrainment in a round jet saturated at about a Reynolds number of 20,000. Thirty nine years after Ricou and Spalding (1961), Dimotakis (2000) observed that in the fully developed flow Re_D*~20,000*, the transition may be traced not to the large scale structures in the flow, which are peculiar to the geometry considered, but rather to the physical significance of the various scales of the turbulence and their Reynolds number scaling. That is, there is a "viscous decoupling of the outer and inner scales of turbulence as responsible for the transition criterion"; however, the relative magnitude of these length scales, while important, do not provide the linkage to the observed effects of initial conditions on the flow. Moreover, to the authors' knowledge, no comparable studies on Reynolds number effects, over the transitional range suggested by Dimotakis (2000), on the velocities in the development region of the jet have been undertaken.

Round free jets, shown schematically in Fig. 1, are part of a large family of free shear flows, which include wakes and mixing layers. They are of interest for their engineering applications as in chemical processes and also because of their fundamental significance as a reference flow. The velocity components in polar co-ordinates *x, r,* and *θ* are denoted *u, v,* and *w* respectively. The terms in the Reynolds decomposition are denoted as *u=U+u'*, etc., where *U* is the mean velocity and *u'* is the fluctuating velocity. At the nozzle, with outlet diameter *D*, the exit mean velocity is denoted by U_j. Along the *x*-axis, the local centerline mean velocity is U_c. Two common characteristic length scales have been used in the literature and represented in Fig. 1 as the jet half-radius $r_{1/2}$ determined by $U_{r_{1/2}} = \frac{U_c}{2}$ and the local time-averaged diameter of the jet denoted by *δ*. Fiedler (1998) divided the jet in to three different regions: *the near-field or potential core* ($0 \leq x / D \leq 6$), *the intermediate-field* and *the far-field or the self-similar* ($x / D \geq 30$). The near and intermediate fields (NIF region) together comprise the developing portion of the jet.

The NIF region, often dominates practical applications of a jet, has received many investigations. The ability to control the flow development in this region would have a vital impact on many engineering applications. Pollard (2008) traced the growth in the ripples that resulted from the Ricou and Spalding (1961) paper and used this as a basis for a research direction that continues to uncover some the fascinating features of this "simple" fluid mechanics problem. He classified these many investigations into three main categories (a) characterization, (b) phase averaged properties and (c) coherent structure identification using minimal spatial and temporal averaging.

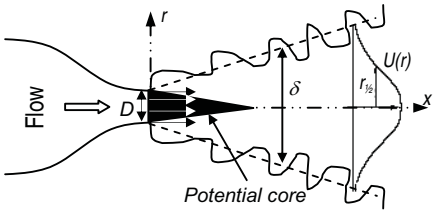

Fig. 1: Schematic of the round free jet and coordinate system.

One of the most dominant and important aspect in the NIF is the mixing transition. For the shear layers, the mixing transition correlated with a transition to three-dimensionality; in the case of jet flows being already three-dimensional even at low Reynolds numbers, such a correlation is not possible. In jets, the mixing transition is associated with the mixing layer region which generates highly energetic large turbulent structures originated from the roll-up in the initial shear layer.

Dimotakis (2000), who linked the outer scale to a variety of other length scales, argued that most shear flows undergo a "mixing transition" to achieve a universal behaviour for the turbulence, and that this mixing transition can be regarded as a universal phenomenon. The minimum Reynolds number required for the mixing transition was $Re_D \approx 20{,}000$. However, the relative magnitude of these length scales does not provide a clear physical reason as to why $Re_D \sim 20{,}000$ is the "magic" criterion that causes the start of the fully-developed turbulent flow.

Fellouah and Pollard (2009), using flying and stationary hot wire measurements, investigated the effect of the Reynolds number on the near and intermediate fields (NIF region) of a round free jet. A significant result was obtained from the velocity spectra, where they were accompanied by the appearance of the inertial subrange for Reynolds numbers above *~20,000* rather than the transition from the inertial sub-range to the dissipation range as indicated by Dimotakis (2000). At Reynolds numbers below the mixing transition, the energy of the large scale turbulence (low wavenumbers or frequencies) proceeds directly to the dissipation range (*-7* slope in the frequency spectra).

In the mixing transition, the nature of the mixing of a scalar was observed to change dramatically near a critical Reynolds number $Re_D \sim 10{,}000-20{,}000$, or a Taylor Reynolds number of $Re_T \sim 100-140$. It would be appropriate to investigate the effect of inlet conditions, by varying Re_D, on the development in the NIF region of a round free jet. Finally, if the mixing transition was reflected in the development of the velocity fields (mean and fluctuating), how was the route to self-similarity affected?

EXPERIMENTAL SET-UP

The experimental setup and techniques used for the measurements described in this paper were well developed in Fellouah and Pollard (2009). One of the benefits of using the flying hot wire (FHW), in which the probes were moved through the fluid at a known velocity, was the reduction of the directional biases due to cross-flow, rectification, and drop-out errors, all of which increase with turbulence intensity. To use the FHW with confidence, the velocity of the probes must be at least equal to back-flow velocities in the flow.

In the current experiment, single and X-wires were mounted on a one meter long aerodynamic sting, which was designed to minimise air drag, and driven by a linear motor system in the three directions. The end of the nozzle has affixed to it a tapered nozzle that ends with a razor-sharp edge (Fig. 2) to avoid the lip thickness. The exit plane of the flow was open so that entrainment into the jet may occur both laterally (in the radial direction) as well as from behind the jet exit plane. The probe was calibrated in the potential core of the jet as its velocity field was uniform over the space occupied by the sensors and prong. The calibration was done before and after each experimental run at a velocity range of *1-26 m/s*.

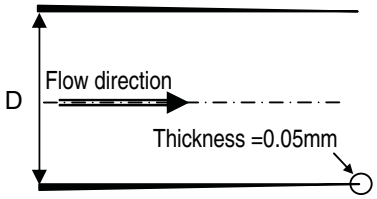

Fig. 2: Shape of the nozzle; *D=8.25 cm*.

PRESENTATION AND DISCUSSION OF RESULTS

Unless noted, those data presented were from the use of stationary hot wires (SHW).

The initial conditions were measured (Fellouah and Pollard 2009) at $x/D = 0.04$ for different Reynolds numbers, and showed clean initial conditions. The exit velocity had a top-hat profile with axial turbulence intensity, less than *3%*, a transverse turbulent intensity, less than *1%*, and the Reynolds shear stress distribution vanishes on the centerline as expected. The development of the axial mean velocities, normalized by the centerline mean velocity, at different axial positions *x/D* was presented in Fig. 3. The profiles were symmetric within measurements uncertainties. The 'top-hat' distribution at the nozzle exit tends to persist to about *5D-6D*. The axial mean velocity profiles at $x/D = 20$ collapse for the two Reynolds number considered. Fig. 4 displays the axial mean velocity decay obtained using both a stationary and flying hot wire. In the current

experiment, *300* traverses were used. These data were ensemble averaged to provide axial mean and turbulence intensity values at every $x/D = 0.5$ position. Figure 4 shows that the centerline axial mean velocity was independent of the Reynolds number and decays linearly downstream beyond $x/D = 6$ with a virtual origin of *2.5* and a decay constant of *5.59*. These values were in good agreement with those reported by Ferdman *et al.* (2000) and Hussein *et al.* (1994). Note that on Fig. 4, the solid line drawn between $x/D \sim 14$ and $x/D \sim 28$ fits the mean of both the flying and stationary hot wire data and the error bars indicate $U_c = \pm 0.05 \frac{U_j}{U_c}$. It was clear that for the axial mean velocity, the stationary and flying hot wire data are the same within experimental uncertainty, including possible sampling limitations with the flying hot wire.

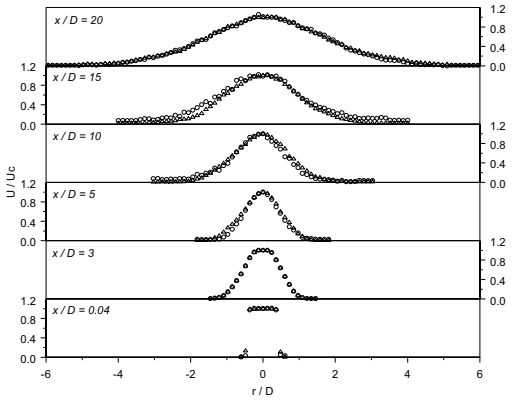

Fig. 3: Streamwise mean velocity at different axial positions. Symbols: Δ *Re$_D$=30,000*, o *Re$_D$=10,000*.

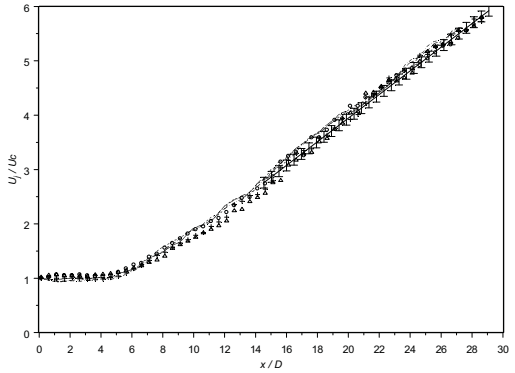

Fig. 4: Axial decay of centerline mean velocity. Line drawn to indicate mean of the data SHW measurements: Δ *Re$_D$=30,000*, o *Re$_D$=10,000*, + *Re$_D$= 6,000*, FHW measurements: - - - *Re$_D$=30,000*, ···· *Re$_D$=10,000*, —·— *Re$_D$= 6,000*.

The longitudinal evolution of the turbulence intensities obtained from the stationary and the flying hot wire along the jet axis ($r/D = 0$), and for the stationary hot wire along a line of constant radius ($r/D = 1/2$), was provided in Fig. 5. The FHW data were seen to be in excellent agreement with the SHW data; the slight disparity between the two sets of data at axial distances $x/D = 15$ was probably due to insufficient sampling in the case of the FHW. The present results were in good agreement with those of Xu and Antonia (2002), Abdel-Rahman *et al.* (1997) and Tong and Warhaft (1994). In the near field region, the turbulence intensities increase due to the large-scale coherent motions that arise in the shear layer. Their influence on the centerline intensities increases as they progress through the potential core and eventually coalesce at the end of the potential core. They then mix as the flow develops towards equilibrium in the far field. The intensities reached the nominally accepted value of about *28%* at $x/D = 30$. The turbulence intensities in the shear layer were higher than at the centerline because the mixing layer generates highly energetic large turbulent structures. The evolution of the structures close to the nozzle exit at $r/D = 1/2$ was due to the initial shear layer instabilities, of the Kelvin-Helmholtz type, which break down into vortical structures with kinetic energies of the order of the mean flow in the layer (Ferdman *et al.* 2000). Immediately downstream of the nozzle exit, the initial turbulence energy decays before it increases again at about *3D* under the effect of the growing large structures. The turbulence intensities in the shear layer ($r/D = 1/2$) were similar in shape to those observed by Burattini *et al.* (2004) for the case of the flow downstream the grids placed at the nozzle exit plane and taken along the jet centerline.

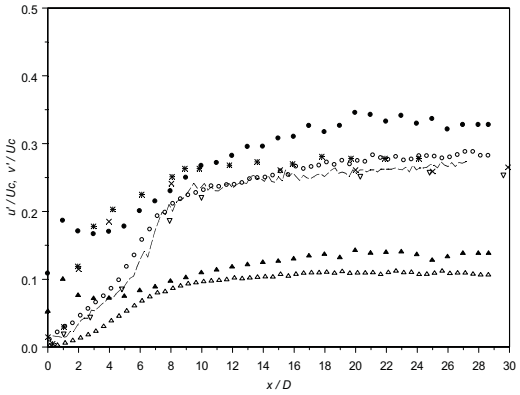

Fig. 5: Evolution of centerline turbulence intensities at *Re$_D$=30,000*. Symbols: o *u'/U$_c$*, Δ *v'/U$_c$*, --- FHW measurements, ∇ *u'/U$_c$* at *Re$_D$=86,000* (Xu and Antonia 2002), × *u'/U$_c$* at *Re$_D$=13,200* (Abdel-Rahman *et al.* 1997), * *u'/U$_c$* at *Re$_D$=140,000* (Tong and Warhaft 1994), no-filled symbols: *r/D=0*, filled symbols: *r/D=½*.

The downstream development of two characteristics of the jet shown in Fig. 6 have a closely constant initial region followed by a region in which their spread increases linearly for $x/D > 10$, with slopes of *0.0969* for the jet half-radius and *0.4125* for the local time-averaged diameter close to 0.096 found by

Panchapasekan and Lumly (1993) for the jet half radius development.

In the next section, the axial and radial evolutions of the one dimensional velocity spectra E_{11} (*u*-velocity spectra), calculated from SHW data, were given for different Reynolds numbers *6,000*, *10,000*, *30,000* and *50,000*. The fast-Fourier-transform algorithm was used to draw these velocity spectra. Note that all velocities spectra were normalized by the Kolmogorov length scale, $\eta_K = \left(\frac{\nu^3}{\varepsilon}\right)^{1/4}$, and Kolmogorov velocity scale, $U_{\eta_K} = (\varepsilon\nu)^{1/4}$. In all velocity spectra figures below, the dotted-lines corresponding to ${k_1}^{-5/3}$ and ${k_1}^{-7}$ (k_1 is the wavenumber in *x*-direction) were also included. The *-5/3* slope is associated with the range of frequencies in which the energy cascade is dominated by inertial transfer, the -3 slope reflects what is expected for two dimensional turbulence, while the *-7* slope characterizes the dissipation range where viscous forces dominate.

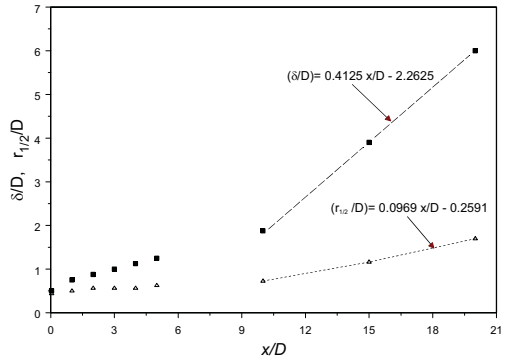

Fig. 6: Axial evolution of the jet width. Discontinue indicates the fit.

The axial velocity spectra, E_{11}, at various *x/D* along the jet axis ($r/D = 0$) was shown in Fig. 7. The spatial development of the spectra clearly indicate that the near field was dominated by shear layer vortex roll-up that eventually evolved to a broad frequency distribution with no discernable frequency peaks. At $x/D = 1$, the velocity spectra displays different shapes with local peaks that reflect the exit conditions. At $x/D = 3$, the velocity spectra evolves to display a turbulence cascade with one pick remaining at Strouhal number *St=0.479* ($St = \frac{fD}{U_j}$) close to *St=0.485* given by Jung *et al.* (2004) (for $x/D = 4$ and *Re$_D$=117,600*) and *St=0.4* given by Mi *et al.* (2001) (for $x/D = 3$ and *Re$_D$=16,000*). This pick was associated with successive pairings of the shear layer instability. At these positions, the formation of coherent structures was apparent with the increased energy content. Within the shear layer region ($r/D = 1/2$), at the same position, this pick disappears and the velocity spectra evolves to what was expected for more fully developed turbulence and displays the *-5/3* and *-7* slopes (Fellouah and Pollard 2009). This value of the Strouhal number was found independent of the Reynolds number which indicates that the Reynolds number had no effect on the number of vortices formed per unit length of jet. Farther downstream the jet (at $x/D = 10 - 20$), the velocity spectra fill out and displays frequency ranges of many decades. In the lower wavenumbers, the intensity of the velocity spectra increases with the axial distance indicating the increase of the energy transfer.

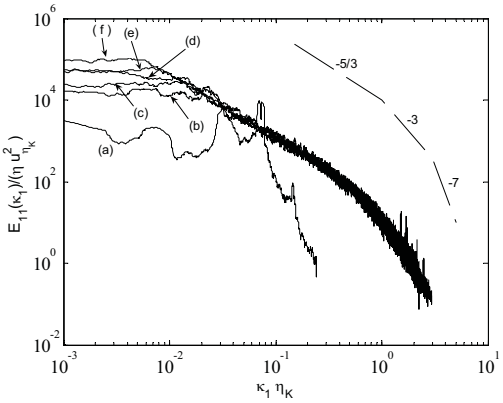

Fig. 7: Velocity spectra of *u* at *r/D=0* and *Re$_D$=30,000*. *(a) x/D=1, (b) x/D=3, (c) x/D=5, (d) x/D=10, (e) x/D=15, (f) x/D=20*.

Figure 8 provides the velocity spectra on the jet centerline for the axial location $x/D = 10$ and for different Reynolds numbers. It was clear that the mixing transition, which demarcates *Re$_D$=10,000* and *Re$_D$=30,000*, displays different spectral energy content. The inertial sub-range, represented by the -5/3 slope, was certainly more evident at *Re$_D$=30,000* and *50,000* than at the lower Reynolds numbers. This result shows that it was the appearance in the inertial sub-range itself that may indicate the mixing transition. The data presented here were taken using the same experimental conditions (save for altering the inlet *Re*), so it was believed the effects of altering the inlet *Re$_D$* were a direct result of the change in the spectra.

Figure 9 shows the *u-spectra* at Reynolds numbers below the mixing transition *30,000*. The axial velocity spectra were calculated at different radial positions represented by r_i in this figure, where r_i correspond to the radial position where $\frac{U}{U_c} = i$, that is r_1 corresponds to the jet axis centerline and r_0 to the outer region of the jet. At $x/D = 10 - 20$, the energy spectrum definitely shows an inertial subrange in all radial positions, which agrees well with the Kolmogorov law. The *-5/3* slope was well developed giving a transition from the inertial subrange to the dissipation subrange. This was the case only at $x/D = 20$ for *Re$_D$=10,000* (Fellouah and Pollard 2009). At the outer region of the jet, all velocity spectra showed only the dissipation subrange as expected due to the final stage of decaying turbulence. From these velocity spectra data, the increase of the Reynolds number and the evolution downstream of the jet favor the appearance of the *-5/3* slope which was a consequence of the appearance of the mixing transition. This was due to the fact that for a given Reynolds number, when moving downstream of the jet, the flow evolves to the fully developed turbulent, or self-similarity region. From this result, it can be concluded that the mixing transition in the jet was a local phenomenon.

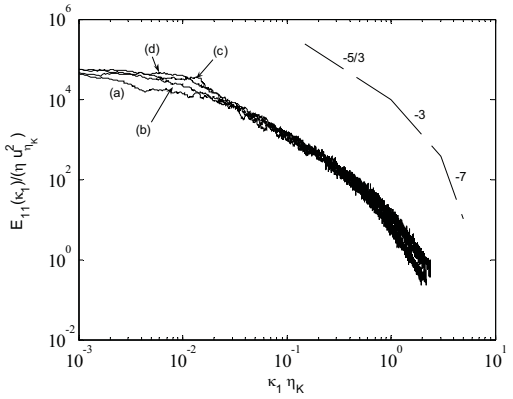

Fig. 8: Velocity spectra of *u* at *r/D=0* at *x/D=10. (a) Re$_D$= 6,000, (b) Re$_D$=10,000, (c) Re$_D$=30,000 and (d) Re$_D$=50,000*

Dimotakis (2000), using the theory presented in Kolmogorov (1941), linked the local time-averaged diameter, δ, to a variety of other length scales: the Kolmogorov length scale η_K, the viscous length scale η_ν , $\eta_\nu = \left(\frac{2\pi}{k_1}\right)$, estimated in terms of the wavenumber k_1, where the energy spectrum deviates from the -5/3 slope which, from the spectra measurements showed here, happens for $k_1\eta_K \approx 1/8$. This value, confirms those found in the literature, see Saddoughi and Veeravalli (1994) who assembled data from a variety of flows for a Taylors Reynolds number $23 < Re_T < 3{,}180$ where $Re_T = \frac{u'\eta_T}{\nu}$, η_T is the Taylor scale, defined as $\eta_T = \left[\overline{u'^2}/\overline{\left(\frac{\partial u'}{\partial x}\right)^2}\right]^{1/2}$. Another length scale considered was the laminar length scale, η_L (as an estimate of the Leipmann-Taylor microscale), defined as $\frac{\eta_L}{\delta} = 5.0Re^{-1/2}$, where *Re* is the local Reynolds number, $Re = \frac{U_c\delta(x)}{\nu}$.

Figure 10 shows the effect of the Reynolds number on these five length scales at different axial positions. It shows that the relation between the different length scales was $\eta_K < \eta_T < \eta_\nu, \eta_L < \delta$ and independent of the Reynolds number. On the other hand the relation between η_L and η_ν was affected by the variation of the Reynolds number: for small Reynolds number close to the nozzle exit, the viscous length scale was smaller than the laminar length scale $\eta_\nu > \eta_L$ and for large Reynolds numbers or axial positions far from the nozzle exit, the viscous length scale was bigger than the laminar length scale, $\eta_\nu \leq \eta_L$. According to Dimotakis (2000), as the Re exceeds *~10,000, the two scales* η_L and η_ν should diverge. This result demonstrates the spatial variability of the length scales along the jet centerline and thus the local nature of the mixing transition.

Dimotakis (2000) concluded that a necessary condition for fully-developed turbulence and the Kolmogorov inertial-range similarity ideas to be applied was the existence of a range of scales that are uncoupled from the large scales, and on the other hand, free from the effects of viscosity. Considering that, the relation $\frac{\eta_L}{\eta_\nu} > 1$ must be verified. In the present data, this ratio was found to vary between 0.487 and 1.326 as provided in Fig. 11. It was clear from these data that the ratio exceeds unity for regions well beyond the potential core of the jet, and rather surprisingly, irrespective of the local Reynolds number, *Re,* at the axial position *x/D=20*.

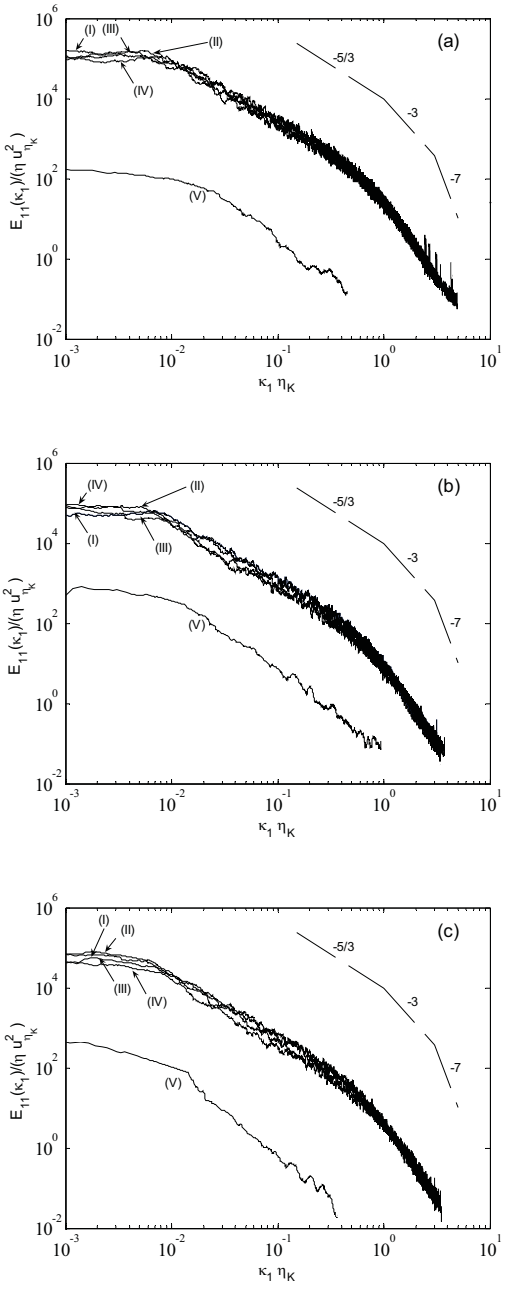

Fig. 9: Velocity spectra of *u* at *Re$_D$=30,000*. (a) *x/D=10,* (b) *x/D=15,* (c) *x/D=20.* (I) r_1, (II) $r_{3/4}$, (III) $r_{1/2}$, (IV) $r_{1/4}$, (V) r_0.

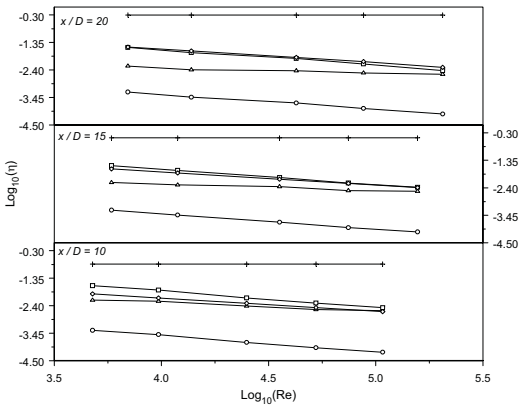

Fig. 10: Reynolds number effect on round jet characteristics at the jet axis. Symbols: o η_K, $\Delta\ \eta_T$, $\Diamond\ \eta_L$, $\Box\ \eta_v$, + δ.

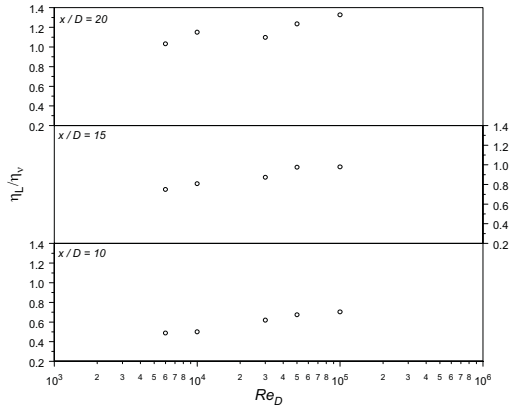

Fig. 11: Effect of the Reynolds number on the variation of the length scale ratio $\frac{\eta_L}{\eta_v}$ on jet centerline.

CONCLUSION

Stationary and flying hot-wire measurements were carried out on the axisymmetric round free jet to explore the mixing transition. Velocity-spectra data revealed that the increase of the Reynolds number increases the range of the wavenumbers that comprise the inertial subrange. The mixing transition was accompanied by the appearance of the inertial subrange given by the *-5/3* slope. At Reynolds numbers below the mixing transition, the energy of the large scale turbulence proceeds directly to the dissipation range. The jet flow development downstream favors the appearance of the inertial subrange. The length scales, Kolmogorov, Taylor and viscous, all decrease in magnitude with the local Reynolds number, *Re*, and the ratio of the laminar to viscous length scales exceeds unity beyond the potential core of the jet. The present data showed that the mixing transition in the jet was a local phenomenon.

REFERENCES

Abdel-Rahman, A.A., Chakroun, W., Al-Fahed, S.F., 1997, "LDA Measurements in the turbulent round jet", *Mechanics Research Communications*, Vol. 24 (3), pp. 277-288.

Burattini, P., Antonia, R.A., Rajagopalan, S., Stephens, M., 2004, "Effect of initial conditions on the near-field development of a round jet", *Experiments in Fluids*, Vol. 37, pp. 56–64.

Dimotakis, P.E., 2000, "The mixing transition in turbulent flows", *Journal of Fluid Mechanics*, Vol. 409, pp. 69-98.

Fellouah, H., and Pollard, A., 2009, "Reynolds number effects within the development region of a round free jet", under construction for publication in *International Journal of Heat and Mass Transfer*.

Ferdman, E., Otugen, M.V., Kim, S., 2000, "Effect of initial velocity profile on the development of the round jet", *Journal of Propulsion and Power*, Vol. 16 (4), pp. 676–686.

Fiedler, H.E., 1998,"Control of free turbulent shear flows", "Flow Control: Fundamentals and Practices", M.G. El-Hak, A. Pollard and J.P. Bonnet Eds, Germany, pp. 335-429.

Hussein, H.J., Capp, S., George, W.K., 1994, "Velocity measurements in a high-Reynolds number, momentum-conserving, axisymmetric, turbulent jet", *Journal of Fluid Mechanics*, Vol. 258, pp. 31–75.

Jung, D., Gamard, S., George, W.K., 2004, "Downstream evolution of the most energetic modes in a turbulent axisymmetric jet at high Reynolds number. Part 1: the near-field region", *Journal of Fluid Mech*anics, Vol. 514, pp. 173–204.

Kolmogorov, A. N., 1941, "Dissipation of energy in locally isotropic turbulence", *Dokl. Akad. Nauk. SSSR 66*, pp. 825.

Mi, J., Nobes, D.S., Nathan, G.J., 2001, "Influence of jet exit conditions on the passive scalar field of an axisymmetric free jet", *Journal of Fluid Mechanics*, Vol. 432, pp. 91–125.

Panchapakesan, N.R., Lumley, J.L., 1993, "Turbulence measurements in axisymmetric jets of air and helium. Part 1: air jet", *Journal of Fluid Mechanics*, Vol. 246, pp. 197–223.

Pollard, A., 2008, "Whither the axisymmetric free jet after 50 years of research?", *International Symposium on Advances in Computational Heat Transfer (ICHMT)*, Marrakech, Morocco.

Ricou, F., and Spalding, D.B., 1961, "Measurements of entrainment by axisymmetric turbulent jets", *Journal of Fluid Mechanics*, Vol. 11, pp. 21-32.

Saddoughi, S. G., and Veeravalli, S. V., 1994, "Local isotropy in turbulent boundary layers at high Reynolds number", *Journal of Fluid Mechanics*, Vol. 268, pp. 333-372

Tong, C., Warhaft, Z., 1994, "Turbulence suppression in a jet by means of a fine ring", Physics of Fluids, Vol. 6 (l), pp. 328-333.

Xu, G., Antonia, R.A.,2002, "Effect of different initial conditions on a turbulent round free jet", *Experiments in Fluids*, Vol. 33, pp. 677–683.